Influence of substrate structure on adhesion behavior of TiN and $TiAl_3$/TiAlN coatings deposited by vacuum arc plasma

E Vardanyan, K Ramazanov, I Yagafarov, V Budilov, R Agzamov

Ufa State Aviation Technical University, Ufa - 450000, Russia

E-mail: vardanyaned@gmail.com

Abstract. This paper presents the study of the influence of a substrate structure on the adhesion behavior of monolayer coatings TiN and multilayer coatings $TiAl_3$ / TiAlN deposited by vacuum arc plasma. Martensitic steel with a coarse-grained (CG) and ultrafine-grained (UFG) structure was used for samples. The samples were subjected to ion nitriding in a glow discharge before coating deposition. Adhesion of the coatings was examined with CSM ScratchTEST. For samples with different structures, critical load was defined at which microcracks are formed in the coatings.

1. Introduction

Durability and reliability of gas turbine engines (GTE) are largely determined by load-carrying capacity of compressor blades. The blades are vital and highly loaded parts that experience considerable alternating and cyclic loads of high frequency during operation. Gas turbine blades typically brake due to erosion, corrosion and fatigue damage [1]. Research of the past two decades showed that mechanical and fatigue properties of metals and alloys can be effectively improved by the formation of UFG nanostructures with submicron and nanocrystalline grains by intense plastic deformation (IPD) [2]. Thus, materials for GTE compressor blades should possess a UFG structure [2]. A promising approach to protect GTE compressor blades is to apply multilayer coatings of periodically arranged nanometer layers of different materials that have high mechanical properties and performance characteristics [3-5]. A range of coatings with different chemical composition (TiN, Ti-Al-N, Ti-C-N, Ti-Zr-N, ZrO_2) and structure (mono- and multilayer) is used to protect GTE compressor blades. Among them multilayer Ti/Al coatings are of great practical interest due to high corrosion resistance in aggressive environments, strength, and low specific weight. The Ti-Al-N system also forms [6,7] a large number of different intermetallic compounds with unique physical and mechanical properties.

One of the most important characteristics of coatings is their adhesion to substrates. Most studies of film deposition analyze not only their structure, phase composition, mechanical characteristics, etc., but also their adhesive properties. Adhesion is commonly assessed by separation of a coating from the substrate and scratching. Separation is mainly applied to thick films, while thin films are typically subjected to scathing [8]. The latter is used in ~70% of applications. While separation defines adhesion in MPa, in scratch tests adhesion is characterized by the critical load at which a film delaminates. ASTM assesses adhesion of coatings against their critical load at which the coating spalls off [9].

The aim of this study is to investigate the influence of martensitic steel structure on the adhesive properties of intermetallic Ti-Al coatings.

2. Experimental approach

Intermetallic Ti-Al coatings were deposited in the installation NNV-6.6-I1. Samples of martensitic steel EI-961Sh were placed in a vacuum chamber. Technological regimes were changed in the following ranges: chamber pressure P = 10^{-1}–10^{-2} Pa; arc current I = 60-120 A; processing time t = 60 min.

The coatings were deposited with simultaneous spraying of one-component cathodes from Al and Ti in the conditions of rotation of the table around its axis. During the deposition, the samples moved through four areas: 1) where the samples were exposed to an Al ion flux; 2) where the samples were exposed to an Al and Ti ion flux (transition area); 3) where the samples were exposed to a Ti ion flux; and 4) where the samples were not exposed to deposition (shadow zone) [9]. The resulting coatings contained different grades of intermetallic phases.

To study the influence of the substrate structure (coarse or ultrafine grain structure) on the adhesion characteristics of the coatings, the samples were exposed to ion nitriding and subsequent deposition of intermetallic Ti-Al coatings onto martensitic steel (see Table 1).

Table 1. Treatment of samples

Sample	Substrate structure and treatment
1	CG + nitriding+ TiN
2	UFG + nitriding + TiN
3	CG + nitriding + $TiAl_3$/TiAlN
4	UFG + nitriding + $TiAl_3$/TiAlN

A CSM Instruments scratch tester [9] (Figures 1 and 2) was used to determine adhesion power and scratch resistance and identify the coating failure mechanism. The surface of the coatings was scratched with a diamond spherical indenter of the Rockwell C type with a curvature radius of 200 mm at a continuously increasing load. A computer was used to register the applied load (F_N, H), the penetration depth of the indenter (Pd, μm) and acoustic emission (AE, dB), which reflected the destruction, delamination or spalling of the coating. After that, the load was released and the indenter moved in the opposite direction to measure the restored scratch depth (Rd, μm). The tests were performed in the following conditions: the indenter was increasingly loaded at 0.3-30 N; the indentation rate was 2 mm/min; the scratch's length was 5 mm; the load application rate was 11.88 N/min; the frequency of the discrete signal was 60 Hz, and the power of the acoustic emission was 9 dB. The minimum (critical) loads LC, at which first cracks appeared, were specified in the tests.

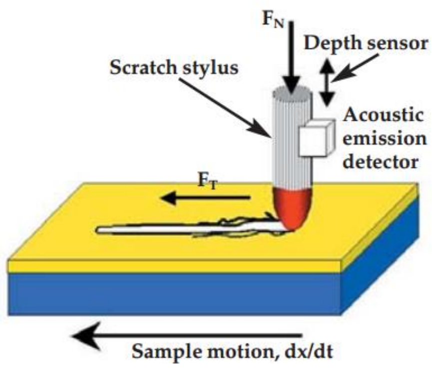

Figure 1. Scratch adhesion test schematic (from ASTM C1624) [9].

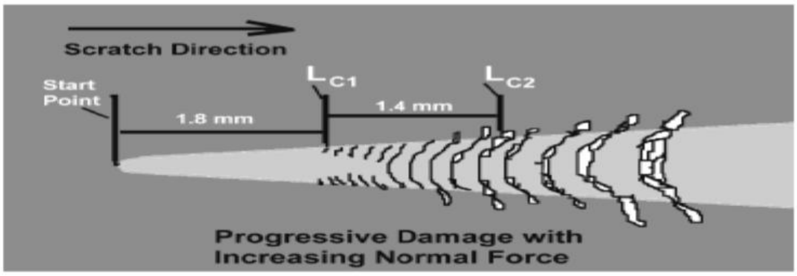

Figure 2. Formation of microcracks at an increasing load [9].

3. Results and discussion

Coating thickness was 10-10.5 µm, while the thickness of individual layers in multilayer coatings $TiAl_3$ / TiAlN was ~ 0.8...1 µm (Figure 3).

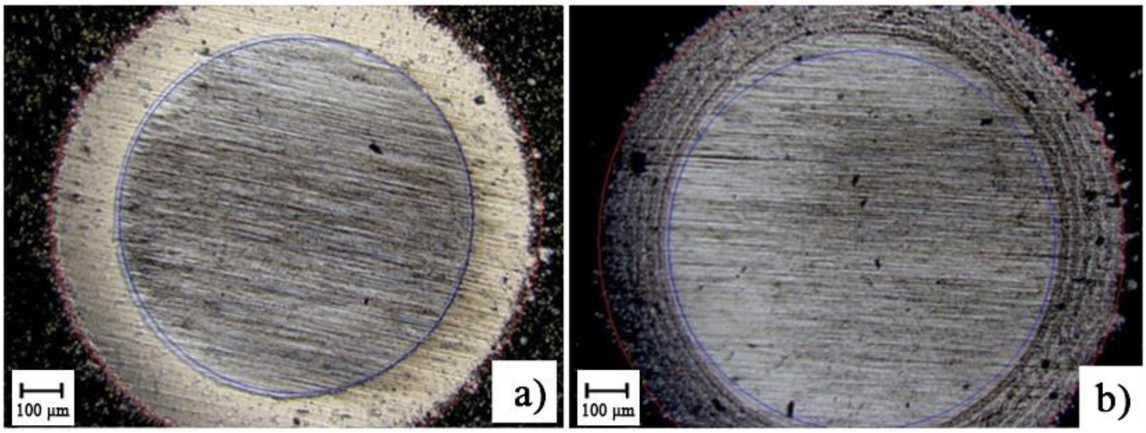

Figure 3. Measurement of coating thickness for a) TiN at 10x magnification; b) $TiAl_3$/TiAlN at 10x magnification.

CG and UFG samples of martensitic steel with TiN and $TiAl_3$/TiAlN coatings processed with different technologies (Table 1) were investigated with sclerometry (Table 1). Optical images of the scratch tracks are shown in Figure 4.

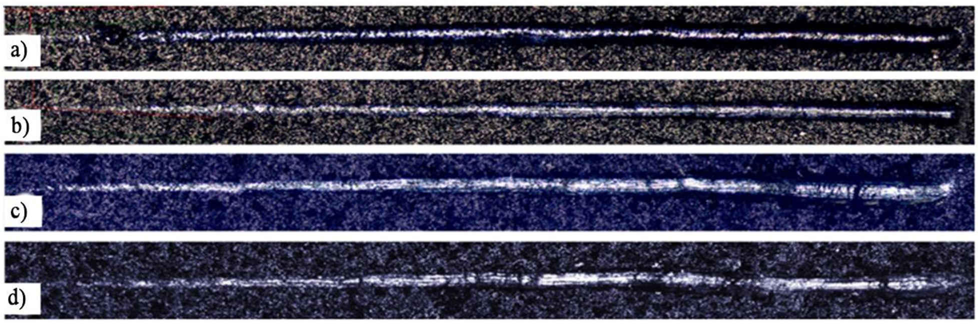

Figure 4. Optical images of the scratch tracks on treated samples: a) CG + ion nitriding + TiN; b) UFG + ion nitriding + TiN; c) CG + ion nitriding + $TiAl_3$/TiAlN; d) UFG + ion nitriding + $TiAl_3$/TiAlN.

The indenter penetration depth is given in Figure 5.

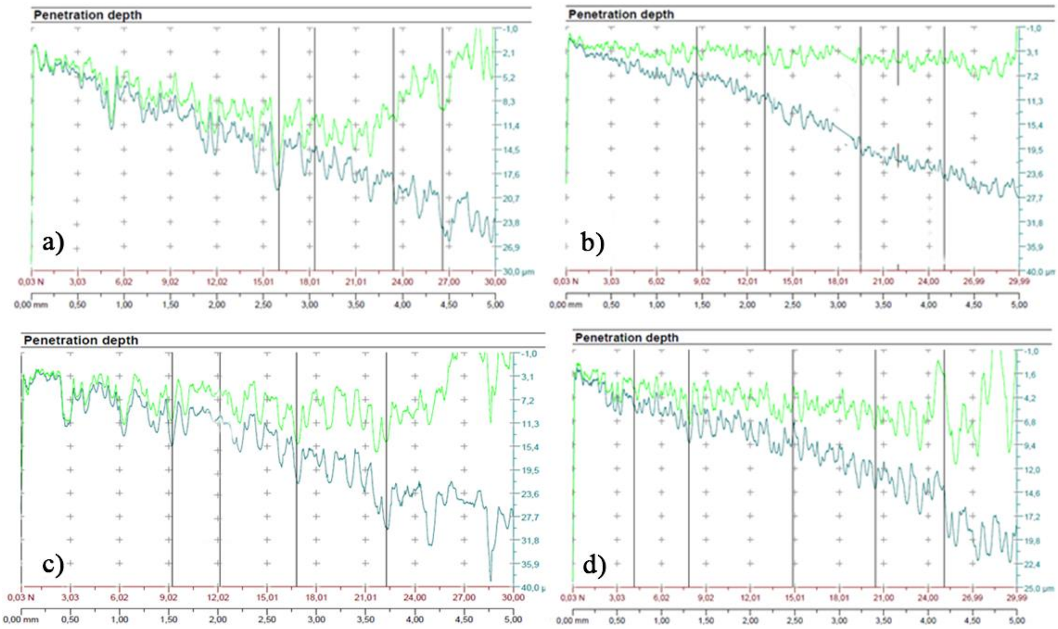

Figure 5. Indenter penetration depth: a) CG + ion nitriding + TiN; b) UFG + ion nitriding + TiN; c) CG + ion nitriding + $TiAl_3$/TiAlN; d) UFG + ion nitriding + $TiAl_3$/TiAlN.

The results show that the indenter penetration depth under the load of 30 N and the scratch depth after the load was released differ during the transition from CG structure (Figures 5a and 5c) to UFG structure (Figures 5b and 5d). Scratching of samples with monolayer TiN coatings showed that the depth of loaded indenter penetration for CG and UFG structure is similar and amounts to ~25-27 µm. However, the track depth after release of the load for samples with the CG structure is about 15 µm, which exceeds the thickness of the coating. Thus, the TiN coatings on the samples with the CG structure destroyed completely. At the same time, the depth of the track after release of the load was 7.5 µm and the coatings remained for the samples with the UFG structure. The diagram for the indenter penetration depth demonstrates that elastoplastic recovery regions in samples with the UFG structure are significantly greater than those in the samples with the CG structure.

The study of the samples with multilayer $TiAl_3$/TiAlN coatings showed that the loaded penetration depth of the indenter is 32 µm and 22 µm for the specimens with the CG and UFG structure, respectively. The measurements after the load release showed that for the samples with CG structure the track depth was about 15 µm, which also exceeds the thickness of the coating. On the contrary, for the samples with UFG structure the depth of the track was about 7 µm.

Scratch tests of the coated samples (Figures 5 and 6) show that the area of the elastic recovery in the samples with the CG structure is significantly narrower than that of the samples with the UFG structure for both TiN and $TiAl_3$/TiAlN coatings. This finding indicates a larger mechanical performance of the samples with the UFG structure. Table 2 gives optical determination of the critical load at which microcracks occur in the coatings.

Table 2. Critical load of microcracks formation

Treatment	1	2	3	4
Critical load [N]	16	19	16.8	22

The study of the samples with the UFG structure of the substrate material coated with TiN and $TiAl_3$/TiAlN showed that microcrack formation starts at the critical load of 19 N and 22 N, respectively.

4. Conclusions

The comparative analysis of the scratch tests carried out for the deposited martensitic steel proved that:

- all samples demonstrate high adhesion to substrates. There is no delamination of the coatings at the maximum load F = 30 N;
- the critical load, at which microcracks are formed is 16-22 N for the samples with the UFG structure. This value is significantly greater than that of the samples with the CG structure (15-19 N) for both types of coatings (TiN and $TiAl_3$/TiAlN).

Thus, the formation of UFG structure in a substrate improves adhesion strength of the coatings.

References

[1] Nihamkin M Sh, Ravens LV, Konev I P 2006 *Bulletin engine* **3** 93
[2] Feuerstein A, Kleyman A 2009 *Surface and Coatings Technology* **204** 1092
[3] HetmaEczyk M, SwadIba L, Mendala B 1996 *Surface Treatment Conference materials, III Nationwide Science Conference* **9** 240
[4] Urbahs A, Savkovs K, Urbaha M, Kurjanovics I 2012 *Nanodevices and Nanomaterials for Ecological Security. NATO Science for Peace and Security Series B: Physics and Biophysics* 307
[5] Zhirkov I, Oks E, Rosen J 2015 *J. Appl. Phys*. **117** 213
[6] Musil J, Stupka P 2015 *Int. J. Nanomanufacturing* **11** 78
[7] Budilov V et al 2004 *Mat. Sci. and Eng A* **375-377** 656
[8] Budilov V, Vardanyan E 2015 *Journal of Physics: Conference Series* **652** 012053
[9] Lunev M, Nemashkalo O 2010 *FIP the PSE* **8**(1) 64
[10] Stephen T, Gonczy A 2005 *Int. J. Appl. Ceram. Technol.* **2** 422

Acknowledgments

The authors are grateful to the Russian Science Foundation for support of this work through the project No. 15-19-00144.